

HIGH-STRENGTH CONCRETE FOR FLEXURAL DESIGN OF BRIDGE GIRDERS

Halit Cenan Mertol, Sami Rizkalla, Paul Zia
North Carolina State University, USA
Amir Mirmiran
Florida International University, USA

Abstract

This paper presents the fundamental characteristics of high-strength concrete in the compression zone of a flexural member and its applicability for the design of the bridge girders. A total of 21 plain concrete specimens were tested under combined flexure and axial compression to evaluate the stress-strain distribution of high-strength concrete in the compression zone of flexural members. The variables considered in this investigation were mainly the strength of concrete (69 to 124 MPa) and the age of the specimen. Two independent loads, concentric and eccentric, were applied to the specimens with a specific configuration to induce maximum strain at one face and zero strain at the other extreme face. A typical specimen had 229x229 mm square cross-section and was 1016 mm long. The measured stress-strain curves and stress block parameters, including the influence of the concrete strength, were compiled with the data in the literature to evaluate the fundamental characteristics of high-strength concrete in the compression zone of flexural members. The results were used to recommend revisions for the AASHTO-LRFD Bridge Design Specifications to extend the current limitation of 69 MPa concrete compressive strength up to 124 MPa.

1. Introduction

The use of high-strength concrete (HSC) has become a common practice worldwide. In bridges, HSC could lead to longer spans and wider spacing of girders, resulting in reduction of the total number of supporting piers, construction time and overall cost of the bridges. Furthermore, the high durability of HSC could reduce the maintenance costs and increase the service life of the bridges. Nevertheless, due to lack of research data, [1] limit the applicability of HSC to 69 MPa. The US National Cooperative Highway Research Program has initiated separate projects to remove this barrier. The main

objective of the research presented in this paper is to recommend revisions to the [1] to extend the applicability of its flexural and compression design provisions for reinforced and prestressed concrete members to concrete strengths up to 124 MPa.

This paper presents the research findings of 21 unreinforced HSC members with target concrete compressive strengths ranging from 69 to 124 MPa, tested under combined axial load and flexure to evaluate the stress-strain distribution in the compression zone of flexural members. Stress-strain curves and stress block parameters for HSC were obtained, evaluated and compiled with the data available in the literature to propose the recommended revisions.

2. Experimental program

2.1. Test specimens

The test series consisted of 21 specimens of 229x229 mm cross-section and 1016 mm overall height. A general view of the concrete test specimen is shown in Figure 1. The end sections of the eccentric bracket specimens were heavily reinforced with transverse reinforcement and confined with rectangular steel tubes, while the test region in the middle of the specimens was 508 mm long plain concrete. The combination of the steel tubes and heavy reinforcement ensures proper transferring of the axial load and moment from the machine to the test region of the specimen and eliminates possible localized failures of the specimens at the ends. The main parameter considered was the concrete strength. Five specimens were tested for a target concrete strength of 69 MPa while six and ten specimens were tested for target concrete strengths of 97 and 124 MPa, respectively. The specimens were cast vertically. Three 100x200 mm cylinders were cast for each specimen to be tested at the testing day. Both the specimens and the cylinders were moist-cured for the first 7 days. They were then stored together in the laboratory environment until testing. The cylinders were ground at both ends to ensure uniformity of the applied axial load.

2.2. Material properties

Mix designs, for the three concrete target strengths, 69, 97 and 124 MPa, were developed after numerous laboratory and plant trial batches by [2]. Details of the concrete mix design for each target strength are given in Table 1.

Table 1 – Three concrete mix designs for target strengths of 69, 97 and 124 MPa [2]

Material	Target Strengths		
	69 MPa	97 MPa	124 MPa
Cement (kg/m ³)	417	417	555
Microsilica Fume (kg/m ³)	44	44	44
Fly Ash (kg/m ³)	114	114	30
Sand (kg/m ³)	625	780	736
Rock (kg/m ³)	1085	1085	1085
Water (kg/m ³)	173	148	158
High Range Water-Reducing Admixture*	1110	1565	2345
Retarding Admixture*	195	195	195
w/cm	0.30	0.26	0.25
28-Day Compressive Strength (MPa)	78.9	99.1	117.8

* mL per 100 kg cementitious materials

2.3. Test method and test set-up

A schematic view of the test set-up is shown in Figure 1. The test concept was based on the test method developed by [3] to simulate the compression zone of a flexural member. The two axial loads, P_1 and P_2 , were adjusted during the test to maintain zero strain (which is at the neutral axis for a flexural member) at one face of the specimen and the maximum compressive strain at the opposite face of the cross-section. The applied load was increased monotonically up to failure. In each loading step, the primary axial load applied by the test machine, P_1 , was applied to induce a constant axial strain in the cross-section. The secondary load applied by the jack, P_2 , was adjusted to maintain zero strain at one face, and produce maximum strain at the opposite face.

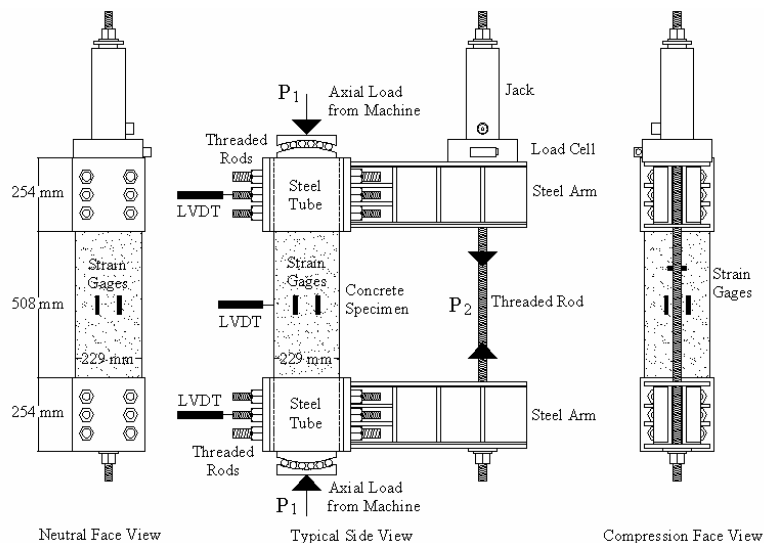


Figure 1 – Test set-up

Two steel brackets were connected to the rectangular steel tubes used at the ends of the specimens. The holes in the steel tubes enabled transfer of the forces from the bracket to the concrete section by threaded rods. Two specially designed roller bearing systems were used at the top and bottom of the specimen to ensure concentric location of the axial load, P_1 , applied to the specimen.

2.4. Instrumentation

The main axial load, P_1 , was applied by a 1000 ton Baldwin-Lima-Hamilton hydraulic compression machine and the applied axial load was measured by a load cell attached to the testing machine. The secondary load, P_2 , was applied by a 60 ton Enerpac hydraulic jack operated manually and the load was measured by a 50 ton Strainsert Universal Flat Load Cell.

Each specimen was instrumented by a total of nine 60 mm electric resistance strain gages. Two strain gages were located on the surface which is designed to be the neutral face. Four gages were mounted on the two sides of the specimen. Three gages were located on the surface of maximum compression strain of the specimen, of which one was used to measure the transverse strain of concrete. Three 25 mm linear variable displacement transducers (LVDT) were placed at the top, bottom and mid-section in order to obtain the deflected shape of the specimen and to incorporate the effect of secondary moment induced by the deformation. The locations of the instrumentations for the test specimens are shown in Figure 1. The applied loads, P_1 and P_2 , stroke of the compression machine, 3 LVDT readings and 9 electric resistance strain gages were recorded during the tests by a data acquisition system.

2.5. Test procedure

The roller bearing systems were placed at the top and the bottom of the specimen to transmit the main axial load concentric to the plain concrete portion of the specimen. The specimen is positioned, aligned and leveled on the roller bearing system at first. A timber frame was then assembled around the specimen to ensure stability of the test set-up and safety at failure. The bottom and top arms were placed and connected to the specimen by using threaded rods. The load cell and the jack, supplying the secondary load, were placed on the top arm. The bottom arm and the top arm assembly were connected to each other by using a 25 mm threaded rod. The top roller bearing system was then positioned and leveled. A thin layer of hydrostone (gypsum cement) was placed between the roller bearing system and the specimen at the top and the bottom.

After leveling of the specimen, the readings from the instrumentation were balanced to zero. As the main axial load started to increase incrementally, the secondary load was applied by a hydraulic jack using a hand-pump to maintain neutral surface (zero strain) at one face of the specimen. The loading rate was approximately 2 microstrains per second at the extreme compression face of the specimen. Each test was completed in approximately 25 minutes. The tests were stopped after the explosive failure of the

concrete in the compression zone. Three companion cylinders were tested before testing each specimen to determine the average compressive strength of concrete.

3. Test results and discussions

A total of 21 specimens were tested for three target concrete strengths, 69, 97 and 124 MPa. However, the average cylinder strengths for each target strength were 76.4, 102.5 and 106.0 MPa, respectively. The highest cylinder strength achieved in this research was 110.6 MPa. All the test specimens had similar explosive failure mode. No cracks were observed up to failure. Typical failure mode for the eccentric bracket tests is shown in Figure 2. The cylinder strength, age at testing, the loading rate and the ultimate compressive strain achieved by the specimens are summarized in Table 2. A typical stress-strain distribution for HSC is shown in Figure 3. The test results indicate that the ultimate concrete compressive strain value of 0.003 specified by the AASHTO LRFD Bridge Design Specification¹ is acceptable for HSC.

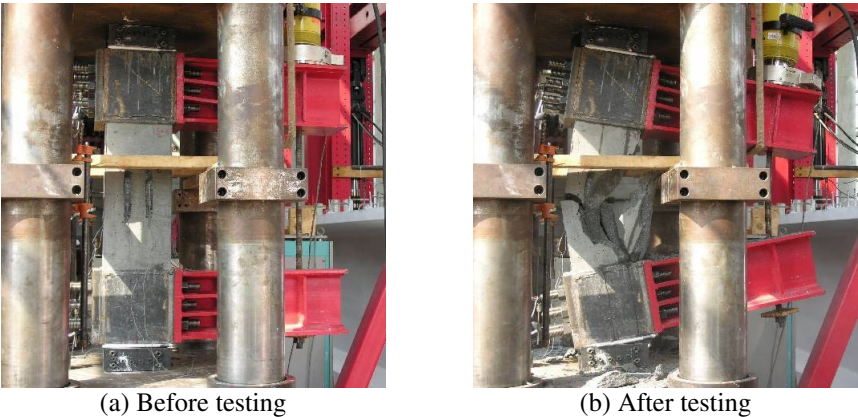


Figure 2 – Typical failure mode for eccentric bracket specimens (18EB6)

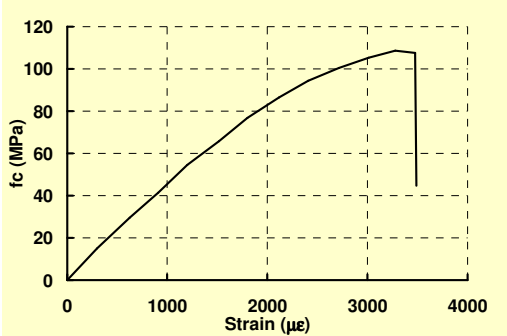


Figure 3 – Typical stress-strain distribution for eccentric bracket specimens (18EB9)

Table 2 – Tabulated test results

Specimen	f'_c at Testing (MPa)	Age at Testing (days)	Loading Rate ($\mu\text{E}/\text{sec}$)	Ultimate Strain (μE)	k_1	k_2	k_3	α_1	β_1
10EB1	76.2	63	12.2	3738	0.65	0.38	1.03	0.90	0.75
10EB2	78.7	109	2.0	3138	0.62	0.36	1.12	0.95	0.72
10EB3	80.7	111	2.4	3407	0.65	0.36	1.14	1.02	0.73
10EB4	71.4	63	2.1	3102	0.64	0.36	1.20	1.06	0.73
10EB5	75.2	62	2.2	3023	0.62	0.36	1.16	1.01	0.72
14EB1	100.9	49	2.3	3316	0.63	0.37	1.00	0.85	0.74
14EB2	98.7	51	1.8	3162	0.60	0.36	1.08	0.85	0.72
14EB3	101.2	52	2.2	3177	0.61	0.36	1.09	0.93	0.71
14EB4	103.7	57	2.3	3032	0.58	0.35	1.10	0.92	0.70
14EB5	105.9	100	5.3	2868	0.57	0.34	1.10	0.92	0.68
14EB6	104.5	101	4.1	2954	0.60	0.35	1.06	0.91	0.69
18EB1	109.1	76	2.2	3684	0.69	0.38	0.82	0.74	0.77
18EB2	110.2	77	2.3	3364	0.67	0.37	0.85	0.77	0.74
18EB3	107.5	81	2.4	2914	0.63	0.37	0.81	0.69	0.73
18EB4	108.7	82	2.6	3306	0.65	0.36	0.88	0.78	0.73
18EB5	110.6	83	2.1	3144	0.65	0.36	0.85	0.76	0.72
18EB6	106.8	84	2.1	3404	0.66	0.37	0.88	0.78	0.74
18EB7	103.7	96	2.5	3585	0.64	0.37	1.05	0.90	0.75
18EB8	99.9	97	2.7	3507	0.65	0.37	1.03	0.91	0.74
18EB9	102.8	99	2.2	3494	0.62	0.36	1.06	0.91	0.72
18EB10	100.7	102	2.0	3532	0.64	0.38	0.97	0.82	0.77

3.1. Stress block parameters

The approach presented by [3] was used to determine the stress-strain relationship and the stress block parameters for each specimen. The details of this approach can be found in [4].

In general, the stress block in the compression zone of a flexure member can be defined by three parameters, k_1 , k_2 and k_3 . The parameter k_1 is defined as the ratio of the average compressive stress to the maximum compressive stress in the compression zone, $k_3 f'_c$. The parameter k_2 is the ratio of the depth of the resultant compressive force, C , to the depth of the compression zone, c . The parameter k_3 is the ratio of the maximum compressive stress in the compression zone to the compressive strength measured by concrete cylinder, f'_c . The design values of the stress block parameters are determined when the strains at the extreme fibers reach the ultimate strain of the concrete, ϵ_{cu} . The three generalized parameters of a stress block can be reduced into two parameters to establish equivalent rectangular stress block using α_1 and β_1 , which assure the same location of the compressive stress resultant at the same location. These parameters are shown in Figure 4. The stress block parameters for each specimen are given in Table 2.

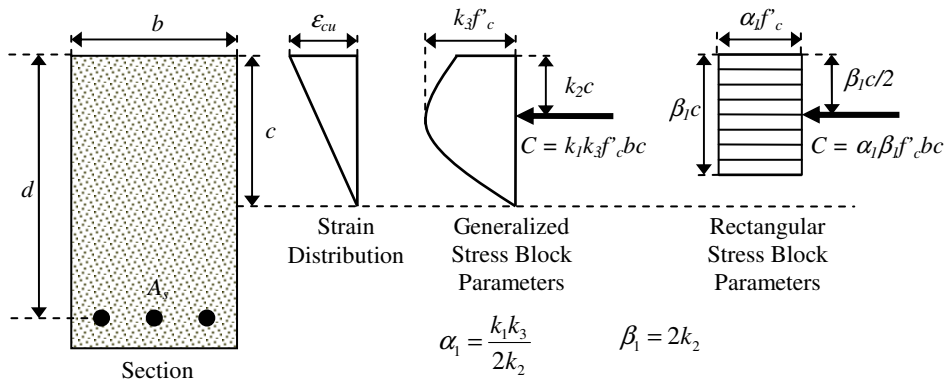


Figure 4 – Stress block parameters for rectangular sections

For normal-strength concrete, the values of k_1 and k_2 , which solely depends on the shape of the stress-strain curve can be derived as 0.85 and 0.425, respectively. The value of k_3 accounts for strain gradient, shape, size, rate of loading and water rise effects of the concrete member compared to the companion cylinder. For normal-strength concrete k_3 was assumed to be 0.85 based on the research conducted by Richart⁵ in 1930s. Therefore, the upper limits for the two rectangular stress block parameters, α_1 and β_1 , can be estimated to be also 0.85. The shape of the stress-strain relationship for HSC tends to approach to a triangular distribution. For perfect triangular distribution of the stresses within the compression zone, the values of k_1 and k_2 would become 0.5 and 0.333, respectively. Assuming a value of 0.85 for k_3 in the case of HSC, the lower bound value for α_1 and β_1 can be established as 0.64 and 0.677, respectively.

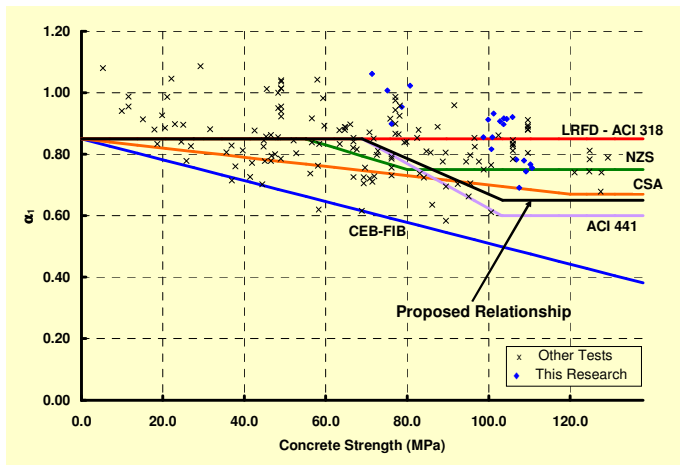


Figure 5 – α_1 relationship for design codes

The calculated values for α_l and β_l are compared with available data in the literature in Figure 5 and Figure 6. The data shown in the figures consist of test results obtained by [3], [6], [7], [8], [9], [10], [11], [12], [13] and this research. The figures include also the current code equations for the parameters α_l and β_l from the [1], [14], [15], [16], [17], [18].

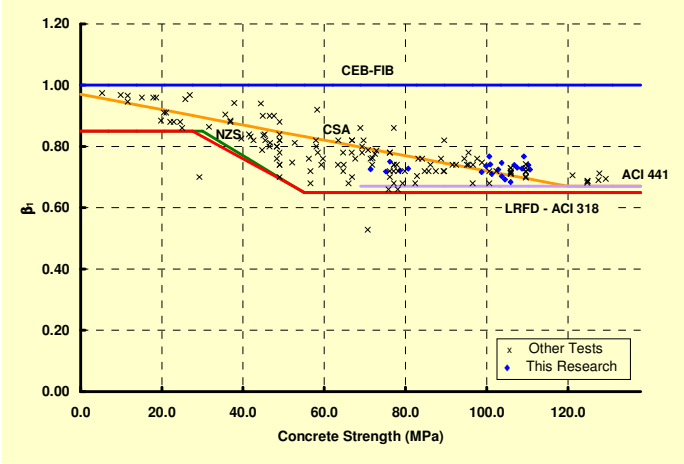


Figure 6 – β_l relationship for design codes

The graph for α_l indicates that as concrete compressive strength exceeds the limit of 69 MPa, α_l tends to decrease. The current value of α_l , 0.85 for all concrete strengths, specified by [1] appears to overestimate the value of α_l for HSC. The following relationship, also presented in Figure 5, is proposed based on the test results in the literature and the research presented in this paper. This relationship would seem appropriate for HSC up to 124 MPa. Note that the upper bound for the parameter α_l is 0.85, for normal-strength concrete and the lower bound for α_l is 0.64, when the stress-strain relationship of HSC becomes almost linear up to failure. The recommended provision for the parameter α_l is:

$$\alpha_l = \begin{cases} 0.85 & \text{for } f'_c \leq 69 \text{ MPa} \\ 0.85 - 0.0058(f'_c - 69) \geq 0.65 & \text{for } f'_c > 69 \text{ MPa} \end{cases}$$

The data for β_l obtained in this research are consistent with the data reported in the literature. The current equation for β_l , 0.65 for $f'_c > 55$ MPa, specified by [1] represents well the lower bound value and should be applicable also for HSC up to 124 MPa.

4. Summary and conclusion

A total of 21 high-strength plain concrete specimens were tested under eccentric compression to simulate the compression zone of a flexural member by varying the applied axial load and moment. The dimensions of the specimens were 229x229x1016 mm and the concrete cylinder strength ranged from 76.2 to 110.6 MPa. The concept developed by [3] was adopted to utilize largest possible specimen size. The measured data was used to determine the fundamental characteristics of the compressive stress distribution in the compression zone of a flexural member. The following are the recommended provisions to extend the current limit of 69 MPa of [1] to 124 MPa:

1. The ultimate concrete compressive strain value of 0.003 specified by [1] is acceptable for HSC up to 124 MPa.
2. The test results, confirmed by other data in the literature, indicate that the stress block parameter α_1 of 0.85 should be reduced where the compressive strength of concrete increases beyond 69 MPa. The recommended value for the parameter α_1 is:

$$\alpha_1 = \begin{cases} 0.85 & \text{for } f'_c \leq 69 \text{ MPa} \\ 0.85 - 0.0058(f'_c - 69) \geq 0.65 & \text{for } f'_c > 69 \text{ MPa} \end{cases}$$

3. The current value of β_1 , 0.65 for $f'_c > 55$ MPa, specified by [1] is appropriate for HSC up to 124 MPa.

5. Acknowledgements

The authors would like to acknowledge the support of the NCHRP through project 12-64 and the Senior Program Officer, David Beal. The authors also thank the contributions of Henry Russell of Henry Russell, Inc. and Robert Mast of Berger/ABAM Engineers, Inc. who serve as consultants for the project. The contribution of Ready Mixed Concrete Company and the personnel of the Constructed Facilities Laboratory are greatly appreciated. The authors would also like to acknowledge the helpful efforts provided by the graduate assistants, Andrew Logan, SungJoong Kim, Zhenhua Wu and WonChang Choi.

6. References

1. AASHTO LRFD Bridge Design Specifications, 3rd Ed, American Association of State Highway and Transportation Officials, (Washington DC, 2004).
2. Logan, A. T., "Short-Term Material Properties of High-Strength Concrete", M.S. Thesis, Department of Civil, Construction and Environmental Engineering, North Carolina State University (Raleigh, NC, Jun. 2005).
3. Hognestad, E., Hanson, N. W. and McHenry, D., "Concrete Stress Distribution in Ultimate Strength Design", ACI Journal 52(4)(Dec. 1955) 455-479.

4. Mertol, H. C., Rizkalla, S., Zia, P. and Mirmiran, A., "Flexural Design of Bridge Girders Using High-Strength Concrete", in "HPC: Build Fast, Build to Last", Proceedings of Concrete Bridge Conference, Nevada, May 2006 (National Concrete Bridge Council, Illinois).
5. Richart, F. E., "Reinforced Concrete Column Investigation", ACI Journal Proceedings 29(Feb. 1933) 275-284.
6. Nedderman, H., "Flexural Stress Distribution in Very-High-Strength Concrete", M.S. Thesis, Civil Engineering Department, University of Texas at Arlington (Dec. 1973).
7. Kaar, P. H., Hanson, N. W. and Capell, H. T., "Stress-Strain Characteristics of High-Strength Concrete", in "Special Publication 55", Douglas McHenry International Symposium on Concrete and Concrete Structures, Michigan, Aug. 1978 (American Concrete Institute, Michigan) 161-185.
8. Kaar, P. H., Fiorato, A. E., Carpenter, J. E. and Corley, W. G., "Limiting Strains of Concrete Confined by Rectangular Hoops", Research and Development Bulletin RD053.01D (Research and Development / Construction Technologies Laboratories, Portland Cement Association, 1978) 1-12.
9. Swartz, S. E., Nikaeen, A., Narayan Babu, H. D., Periyakaruppan, N. and Refai, T. M. E., "Structural Bending Properties of Higher Strength Concrete", in "Special Publication 87" High-Strength Concrete, Sept. 1985 (American Concrete Institute, Michigan) 145-178.
10. Pastor, J. A., "High-Strength Concrete Beams", Ph.D. Thesis, Department of Civil Engineering, Cornell University (Ithaca, New York, Jan. 1986).
11. Schade, J. E., "Flexural Concrete Stress in High-Strength Concrete Columns", M. S. Thesis, Civil Engineering Department, the University of Calgary (Calgary, Alberta, Canada, Sept. 1992).
12. Ibrahim, H. H. H. and MacGregor, G., "Modification of the ACI Rectangular Stress Block for High-Strength Concrete", ACI Structural Journal 94 (1)(Jan.-Feb. 1997) 40-48.
13. Tan, T.H. and Nguyen, N. B., "Flexural Behavior of Confined High-Strength Concrete Columns", ACI Structural Journal 102 (2)(Mar.-Apr. 2005) 198-205.
14. ACI Committee 318, "Building Code Requirements for Structural Concrete (ACI 318-02) and Commentary (318R-02)", (American Concrete Institute, Farmington Hills, Michigan, 2002).
15. ACI Committee 441, "High-Strength Concrete Columns: State of the Art (ACI 441R-96)", (American Concrete Institute, Michigan, 1996).
16. New Zealand Concrete Structures Standards (NZS 3101), (New Zealand Standards, 1995).
17. Canadian Standards Association, "Design of Concrete Structures, CSA A23.3 1994", (Rexdale, Ontario, 1994).
18. CEB-FIB Model Code 1990, Thomas Telford Services Ltd., (London, for Comité Euro-International du Béton, Laussane, 1993).